

Role of protein degradation in growth laws

Ludovico Calabrese^{1*}, Jacopo Grilli², Matteo Osella³, Christopher P Kempes⁴, Marco Cosentino Lagomarsino^{1,5,6*}, Luca Ciandrini^{7*}

1 IFOM Foundation, FIRC Institute for Molecular Oncology, via Adamello 16, Milan, Italy

2 The Abdus Salam International Centre for Theoretical Physics (ICTP), Str. Costiera 11, 34151 Trieste, Italy

3 Physics Department, University of Turin and INFN, via P. Giuria 1, 10125 Turin, Italy

4 The Santa Fe Institute, Santa Fe, NM, United States

5 Dipartimento di Fisica, Università degli Studi di Milano, via Celoria 16, Milan, Italy

6 INFN sezione di Milano, via Celoria 16, Milan, Italy

7 Centre de Biologie Structurale (CBS), CNRS, INSERM, Univ Montpellier, Montpellier 34090, France

✉ These authors contributed equally to this work.

* For correspondence: ludovico.calabrese@ifom.eu (LCa); marco.cosentino-lagomarsino@ifom.eu (MCL); luca.ciandrini@umontpellier.fr (LCi)

Abstract

Growing cells adopt common basic strategies to achieve optimal resource allocation under limited resource availability. Our current understanding of such “growth laws” neglects degradation, assuming that it occurs slowly compared to the cell cycle duration. Here we argue that this assumption cannot hold at slow growth, leading to strong qualitative consequences. We propose a simple framework showing that at slow growth protein degradation is balanced by a fraction of “maintenance” ribosomes. Through a detailed analysis of compiled data, we show how this model is predictive with *E. coli* data and agrees with *S. cerevisiae* measurements. Intriguingly, model and data show an increased protein degradation at slow growth, which we interpret as a consequence of active waste management and/or recycling. Our results highlight protein turnover as an underrated factor for our understanding of growth laws across kingdoms.

Introduction

“Growth laws” (Scott and Hwa, 2011; Kafri et al., 2016) are quantitative relationships between cell composition and growth rate. They uncover simple underlying physiological design principles that can be used to predict and manipulate cell behavior. One of these laws, sometimes called the “first growth law”, relates steady-state growth rate to ribosome allocation and reflects the fact that the biosynthetic rate is set by the fraction of ribosomes that translate other ribosomes (Scott et al., 2010; Metzger-Raz et al., 2017). Specifically, the mass fraction ϕ_R of ribosomal proteins in the proteome increases linearly with growth rate λ , independently of nutrient source.

Fig. 1 provides a visual summary of the relation $\phi_R(\lambda)$. Importantly, there is an empirical offset in this law $\phi_R(\lambda = 0) \neq 0$, i.e., the relationship extrapolates to a nonzero

fraction of ribosomes at zero growth. The presence of an offset seems to be widespread across species (Fig. 1 - Supplement 1). This offset is commonly interpreted using the assumption that only a fraction of the total number of ribosomes (sometimes called “active ribosomes”) is translating and thus producing mass (Scott et al., 2010; Dai et al., 2016). However, no currently available experimental method is able to quantify active ribosomes, and the origin and nature of the inactive ribosomal pool is under debate (Dai and Zhu, 2020). In *E. coli*, deviations from this law at slow growth were explained by a growth-rate dependent fraction of active ribosomes (Klumpp et al., 2013; Dai et al., 2016).

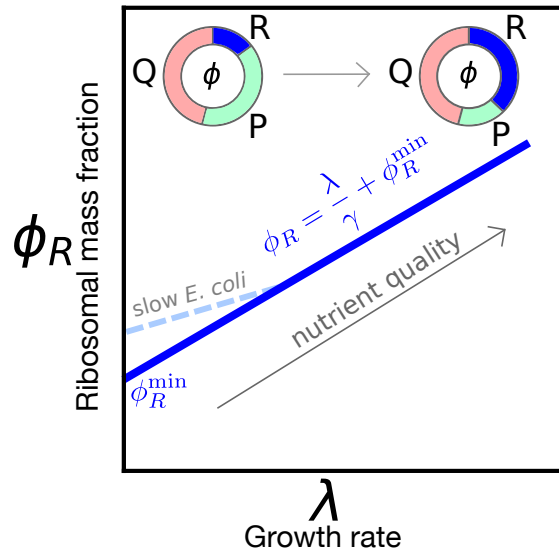


Fig 1. Sketch of the growth law relating ribosome mass fraction ϕ_R to growth rate λ . The fraction of ribosomal and ribosome-affiliated proteins (R) increases with increasing nutrient quality at the expense of the sector of metabolic proteins (P), while a fraction of the proteome (Q) including for instance negatively autoregulated housekeeping genes, is growth rate-independent. Available data for most organisms show a nonzero intercept $\phi_R^{\min} > 0$ (see Fig. 1 - Supplement 1). In *E. coli* (Dai et al., 2016), the law deviates from linearity at slow growth ($\lambda \leq 1 \text{ h}^{-1}$), making the intercept ϕ_R^{\min} larger.

Protein degradation and turnover are typically neglected in the frameworks describing growth laws (Scott et al., 2010). Clearly if degradation time scales fall in the range of 10-100 h (Goldberg and Dice, 1974; Maurizi, 1992), they are negligible compared to protein dilution by cell growth when nutrients are abundant. However, when the population doubling time overlaps with the typical time scale of protein degradation, the balance between protein production and protein degradation must clearly impact growth (Maitra and Dill, 2015; Kempes et al., 2016; Santra et al., 2017). Importantly, prolonged slow- or null-growth regimes are of paramount importance in the lifestyle of most bacteria (Kempes et al., 2017; DeLong et al., 2010; Long et al., 2021; Gray et al., 2019; Schink et al., 2019; Biselli et al., 2020), as well as in synthetic biology applications (Borkowski et al., 2016). Notably, the smallest bacterial species not only grow slowly but have a small number of macromolecules (e.g. ≈ 40 ribosomes) suggesting that protein turnover matters in slow growth contexts (Kempes et al., 2016).

Here, we propose and explore a generic framework to describe the first growth law including the role of protein degradation and turnover (Kempes et al., 2016; Santra et al., 2017). We first derive the law from basic flux-balance principles. We then falsify on general grounds a scenario where degradation is not accounted for. Finally, we use our framework on *E. coli* and *S. cerevisiae* data, finding that data and model converge on a

scenario of accelerated protein turnover at slow growth.

Results

Degradation sets an offset in the first growth law

We start by formulating a simple theory for the first growth law that includes degradation. The law can be derived from the following total protein mass (M) flux balance relation, valid for steady exponential growth,

$$\lambda M = J_{\text{tl}} - J_{\text{deg}} . \quad (1)$$

Here, λ is the cellular growth rate, J_{tl} is the flux of protein mass synthesized by translation, and we explicitly considered the flux of protein degradation J_{deg} . The term J_{tl} is proportional to the ribosome current $v\rho$ on a transcript, given by the product between the ribosome speed v and its linear density ρ on an mRNA. This quantity corresponds to the protein synthesis rate if the ribosomal current along a transcript is conserved, i.e. if ribosome drop-off is negligible. We assume that ribosome traffic is negligible, therefore the speed v is independent of ρ and can be identified with the codon elongation rate k (Li, 2015). In this model, free ribosomal subunits are recruited to mRNAs and become translationally active via a first-order reaction that depends on the concentration of free ribosomes (Fig. 2a).

A simple estimate (see Box 1) shows that $J_{\text{tl}} = m_{\text{aa}}kR$, where m_{aa} is the typical mass of an amino-acid and R the total number of ribosomes. The flux of protein degradation is determined by the degradation rate η . We first assume that η is a constant that does not depend on the growth rate and it is identical for all proteins, which gives $J_{\text{deg}} = \eta M$.

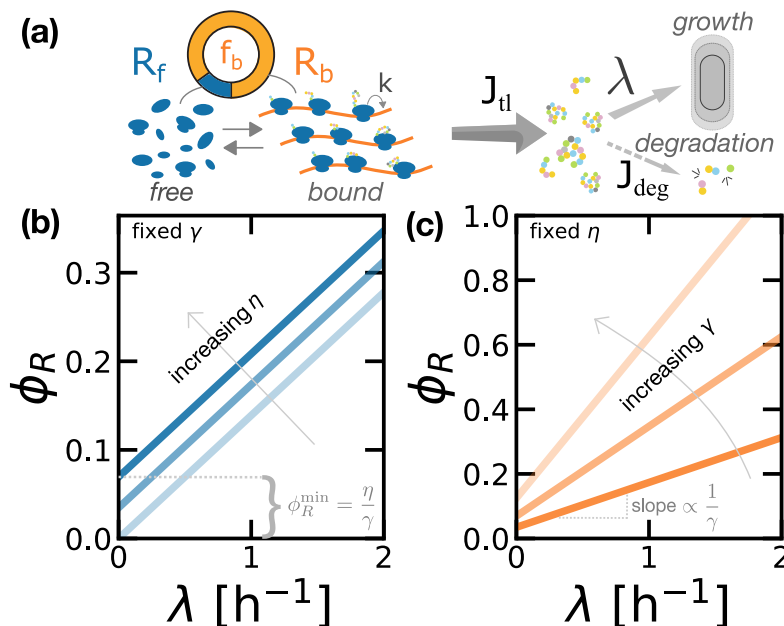


Fig 2. Protein degradation determines an offset in the first growth law. (a) Sketch of the model proposed here, including degradation. (b) The law $\phi_R(\lambda)$ predicted by Eq.(1) shows an offset $\phi_R^{\text{min}} = \eta/\gamma$. The offset increases linearly with degradation rate η at a constant ribosome production rate γ . (c) Varying γ also changes ϕ_R^{min} but it also affects the slope of $\phi_R(\lambda)$. Panel (b) reports $\phi_R(\lambda)$ for $\gamma = 7.2 \text{ h}^{-1}$ and $\eta = 0, 0.25, 0.5 \text{ h}^{-1}$. Panel (c) fixes $\eta = 0.25 \text{ h}^{-1}$ and varies $\gamma = 2, 3.6, 7.2 \text{ h}^{-1}$.

This assumption can be relaxed to study the role of protein-specific degradation rates (see Methods and Materials), but in this work we limit our investigation to the average values of these quantities. Using the expressions for J_{tl} and J_{deg} into Eq. (1) and introducing the parameter $\gamma := k/L_R$ (where L_R is the number of amino acids in a ribosome), we find a simple relation between the ribosomal protein mass fraction ϕ_R and the growth rate λ that involves the degradation rate,

$$\lambda = \gamma\phi_R - \eta. \quad (2)$$

Note that γ can be interpreted as the inverse of the time needed to translate all the amino-acids needed to build a ribosome. If ribosome speed is growth-rate dependent (Klumpp et al., 2013), γ is itself a function of λ . We will come back to this point in the following.

Equation (2) gives an alternative formulation of the first growth law. Crucially, this equation predicts an offset $\phi_R^{min} = \phi_R(\lambda = 0) = \eta/\gamma$ in the law, which we can compare to the experimental range of observed offsets, $\phi_R^{min} \sim 0.02 - 0.1$ (Scott et al., 2010; Metz-Raz et al., 2017). Taking $\gamma \approx 3.6 - 7.2 \text{ h}^{-1}$, this simple estimate returns values for the degradation rate η that correspond to a range of (mean) protein half-lives $\sim 1 - 10$ h. Hence, protein turnover should become relevant for slowly growing cells, when their doubling time falls in the same range of time scales (or is longer). Figure 2 summarizes this result and shows how different degradation rates set different offsets in the predicted linear relationship $\phi_R(\lambda)$. In this framework, the offset $\phi_R^{min} = \eta/\gamma$ can be interpreted as the ratio between the time needed for a ribosome to synthesize a new ribosome and the time scale of protein degradation (or decay), which fixes the size of the ribosome pool in steady growth. In other words, the offset ϕ_R^{min} can be interpreted as the mass fraction of "maintenance ribosomes", which are needed to sustain protein synthesis in resource-limited conditions.

Box 1. The first growth law in the degradation model.

At steady growth, mass balance imposes that the fluxes of mass production J_{tl} and degradation J_{deg} should be equal

$$\frac{dM}{dt} = \lambda M = J_{tl} - J_{deg}. \quad (3)$$

The biosynthesis flux is proportional to j_m , the overall translation rate of the typical transcript, $J_{tl} = m_p N_m j_m$, where m_p is the mass of the typical protein, and N_m is the number of transcripts. Assuming a small translation initiation rate, and thus a low ribosome density on each transcript (Ciandrini et al., 2013), the overall translation rate is $k\rho$, and following (Shaw et al., 2003) the density of ribosomes is

$$\rho = \frac{\frac{\alpha}{k}}{1 + (\ell - 1)\frac{\alpha}{k}}, \quad (4)$$

where ℓ is the size of the ribosome in units of codons (i.e. $\ell \approx 10$) and α is the translation initiation rate. Since initiation is about two order of magnitudes slower compared to elongation, (0.1 vs 10 s^{-1}) (Ciandrini et al., 2013), the density can be approximated as $\rho \approx \alpha/k$. Describing initiation as a first-order chemical reaction, $\alpha = \alpha_0 c_f$, with c_f being the concentration of free ribosomes in solution. Considering that the total number of ribosomes is given by $R = R_b + R_f$, we obtain the following

relation between R_f and R (Greulich et al., 2012)

$$R_f = \frac{kR}{k + Lc_m\alpha_0}, \quad (5)$$

where we have introduced the concentration of transcript c_m . In this theory, the quantity $f_b = R_b/R$ describes the fraction of bound and translating ribosomes. If the total expected time to elongate a typical protein $\tau_e = L/k$ is large compared the time that a ribosome remains unused in the cytoplasm $\tau_i = 1/\alpha_0 c_m$, then $j_m \simeq k\rho = \alpha_0 c_f \simeq kR/(LN_m)$, and the mass production term reads

$$J_{tl} = m_{aa}kR. \quad (6)$$

The contribution of protein turnover to the mass balance is $J_{deg} = \eta M$. Thus, by using the relations for J_{tl} and J_{deg} in Eq. (1) we obtain $\lambda = \gamma\phi_R - \eta$ - Eq. (2) in the text. We remind that $\phi_R = M_R/M$ where $M_R = m_R R$ is the total mass of ribosomal proteins and m_R the protein mass of a single ribosome, and that $\gamma = k/L_R$ where $L_R = m_R/m_{aa}$ is the number of amino acids in a ribosome. The quantity γ^{-1} can hence be interpreted as the typical time needed for a ribosome to duplicate its protein content.

The standard framework for the first growth law neglects protein turnover

To illustrate how the framework involving protein degradation provides an alternative (but possibly complementary, see below) interpretation of the players generating the first growth law, we now discuss the more standard derivation of the relationship $\phi_R(\lambda)$. The standard framework neglects protein turnover in all regimes and assumes that only a fraction f_a of ribosomes actively translates the transcriptome, while the remaining subset of ribosomes does not contribute to protein synthesis. Thus, among the total number R of ribosomes, R_i are considered as *inactive*, and only $R_a = f_a R$ *active* ribosomes elongate the newly synthesized proteins with rate k per codon and generating a mass flux J_{tl} . It is yet experimentally unfeasible to distinguish between active and inactive ribosomes (Zhu et al., 2020), and growth laws are typically formulated in terms of the total ribosome to total protein mass fraction ϕ_R . After a few rearrangements (see Box 2), we write

$$\lambda = \gamma(\phi_R - \phi_R^i) = \gamma\phi_R f_a, \quad (7)$$

where ϕ_R^i is the mass protein fraction of inactive ribosomes and $f_a = (1 - R_i/R)$ is the fraction of actively translating ribosomes, which is in principle a function of the growth state λ . Note that all inactive ribosomes are considered as they were sequestered in this model, differently from the pool of cytoplasmic ribosomes introduced in the previous section, which are not translating but follow an equilibrium binding kinetics with transcripts, see Fig 2(a).

The active ribosomes framework predicts an offset in the linear relation $\phi_R(\lambda)$, which originates from the fraction of inactive ribosomes ϕ_R^i at zero growth. When mass is not produced ($\lambda = 0$), in this model there are no ribosomes that are actively translating proteins, but there exists a non-vanishing fraction of inactive ribosomes. Note that Eq.(2) from the “degradation” model, and Eq.(7) from the “active ribosomes” model are mathematically equivalent if we identify the degradation rate η in the first model with the product $\gamma\phi_R^i$ in the second. Hence, the two frameworks give a different interpretation of the mechanisms generating the offset in the ribosomal fraction at vanishing growth.

Box 2. Active ribosomes model

Assuming balanced exponential growth, all cellular components accumulate at the same rate λ . Neglecting protein turnover, the exponential increase of the total protein mass M is

$$\frac{dM}{dt} = \lambda M. \quad (8)$$

The mass production term is usually expressed as the product between the number of actively translating ribosomes R_a , the codon elongation rate k and the mass of an amino acid m_{aa} (Dai et al., 2016):

$$\frac{dM}{dt} = m_{aa} k R_a. \quad (9)$$

Equations (8) and (9) lead to a relation between the growth rate λ and the mass fraction of R_a . However, the number of actively translating ribosomes R_a is not easily accessible experimentally. Instead, one can express it in terms of the total number of ribosomes, $R = R_i + R_a$, where R_i is the number of inactive ribosomes. This gives

$$\lambda = \gamma(\phi_R - \phi_R^i) = \gamma\phi_R f_a(\lambda), \quad (10)$$

which gives an offset in the first growth law, related to the fraction of active ribosomes $f_a(\lambda)$.

Analysis of the slow-growth regime supports a scenario where protein degradation cannot be neglected

We now argue on general grounds that protein turnover must be included in a description of growth laws of slowly-growing cells. To this aim, we compare more closely the two models (Fig. 3 and 3 - Supplement 1). The active ribosomes model (Box 2 and Fig. 3 - Supplement 1) predicts that the fraction f_a is always less than 1 and it adapts to the growth state. Assuming that the fraction of active ribosomes f_a is also a function of λ , one obtains the relationship

$$f_a(\lambda) = \frac{\lambda}{\gamma(\lambda)\phi_R(\lambda)}. \quad (11)$$

Since $\phi_R(\lambda)$ must be finite for vanishing growth rates, Eq. (11) implies that the fraction of active ribosomes must disappear, unless the protein synthesis rate $\gamma(\lambda)$ falls linearly to zero. This prediction appears contradictory, as it suggests the existence of a pool of residual actively translating ribosomes at arrested protein production. Conversely, it seems reasonable to expect that for maintenance purposes the translation elongation rate γ could be nonzero for growth rates comparable to the time scales of protein degradation. In the case of *E. coli*, for example, the measured elongation rate k is different from zero at vanishing growth rate (Dai et al., 2016); given the observed nonzero ϕ_R^{\min} , the theory would predict the complete absence of active ribosomes, in contrast with the experimental measure of a finite translation elongation rate.

Instead, the degradation model implicitly assumes that all bound ribosomes are active and contributing to mass production. In this case, the theory predicts that for vanishing growth rate a pool of "maintenance ribosomes" $\phi_R^{\min} = \eta/\gamma$ counterbalances protein degradation. We also note that in bacteria maintenance protein synthesis is reported to be active even in stationary phase (Gefen et al., 2014). These considerations suggest that, while combined scenarios are possible (see below), and inactive ribosomes might

also play a role, protein turnover should not be neglected in a theoretical description of the determinants of the first growth law and the origin of the offset ϕ_R^{min} .

In *E. coli*, the scenario including protein turnover correctly predicts an increase of degradation rate in slow-growth conditions

In the case of *E. coli*, it is possible to perform a more detailed analysis. The data present a further complication, as direct measurements of protein elongation rate show that this parameter decreases with decreasing growth rate (Dai et al., 2016). Specifically, the elongation rate k shows a plateau ($k = 16 - 17$ aa s⁻¹, $\gamma \sim 8$ h⁻¹) in nutrient-rich growth conditions ($\lambda > 1$ h⁻¹), but elongation slows down in poor nutrient conditions, and reaches a value of ~ 8 aa s⁻¹ ($\gamma \sim 4$ h⁻¹) at vanishing growth (stationary phase). Thus, γ in Eq. (2) and (7) should be considered as functions of λ . Consequently, at slow growth, the first growth law $\phi_R(\lambda)$ deviates from linearity (Dai et al., 2016), as also shown in the sketch in figure 1.

Using this observation, and using the active ribosomes model, Dai and coworkers predicted the fraction of inactive ribosomes. Specifically, Equation (7), informed by the experimental values of ϕ_R , γ and λ , determines f_a from Eq. (11). As discussed above, however, this theory predicts that active ribosomes become vanishing as growth rate decreases. Indeed, the estimated active ribosome fraction f_a obtained following this procedure drops to zero for vanishing λ (red circles in Figure 3 - Supplement 1). Unfortunately, a direct experimental validation of $f_a(\lambda)$ is currently unavailable (Zhu et al., 2020).

When introducing the degradation model, we previously assumed that the degradation rate was a constant. However, η can in principle be a function of the growth state. Assuming the degradation model -Equation (2)- and paralleling the analysis by Dai and coworkers, we derived from the data a protein turnover rate η that depends on λ , as it follows

$$\eta(\lambda) = \gamma(\lambda) \phi_R(\lambda) - \lambda. \quad (12)$$

The estimated degradation rate, assuming this model, is plotted in Fig. 3. In order to validate this prediction, we searched the literature for datasets of protein degradation rates under different nutrient conditions. Despite of the burst of recent quantitative experiments connected to the discovery of growth laws, there are no recent systematic and quantitative measurements of protein degradation in *E. coli*, but many such measurements are available from classic studies (Goldberg and Dice, 1974; Maurizi, 1992; Pine, 1970; Nath and Koch, 1971; Pine, 1973; Mosteller et al., 1980; Larrabee et al., 1980; Schroer and St. John, 1981). The most comprehensive summary is found in ref. (Pine, 1973), therefore we mined these data for average degradation rates (there are variations in protein-specific degradation rates (Mosteller et al., 1980; Larrabee et al., 1980; Schroer and St. John, 1981), which we did not consider here).

Figure 3 shows that experimentally the protein degradation rate varies with the growth rate of the medium in all the *E. coli* strains considered by (Pine, 1973) (see also Fig. 3 - Supplement 2 for other data we compiled). The model prediction shows a good quantitative agreement with the direct measurements on two main levels. First, the degradation rate η increases with decreasing growth rate, and second, the time scales of protein turnover become comparable to dilution at slow growth. This analysis confirms the idea that protein turnover is the driver of the deviation from the linear growth laws at slow growth.

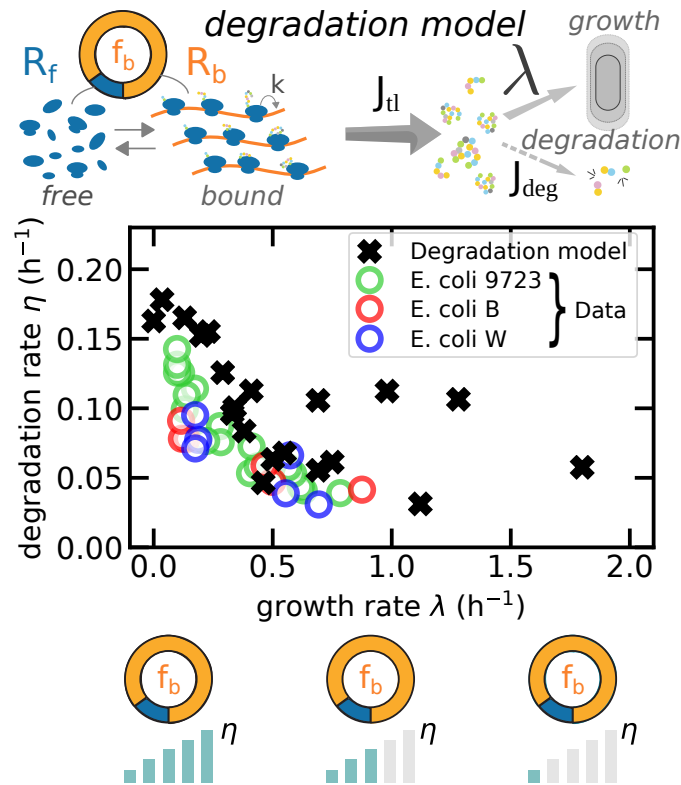


Fig 3. In *E. coli*, the degradation framework correctly captures the trend of measured degradation rates. In the model proposed here (the sketch in the top panel is the same as in Fig. 2a, repeated to facilitate reading) ribosomes follow a first-order kinetics to bind the transcripts, and all bound ribosomes contribute to protein synthesis (mass production). Mass can be lost by protein degradation or diluted by cell growth. The plot reports the estimated *E. coli* degradation rate η assuming this model (cobalt blue circles) and using data from (Dai et al., 2016), compared to experimental data on degradation rate from (Pine, 1973) (other symbols).

In *S. cerevisiae*, ribosome allocation data are compatible with the predictions of the protein turnover model

The available data on yeast do not allow a stringent analysis comparable to the one we performed for *E. coli*. Firstly, they lack data points at slow growth rates for ribosome allocation (Metzl-Raz et al., 2017), as well as precise measurements of translation rates –comparable to the analysis of (Dai et al., 2016). Secondly, degradation data are not as abundant.

However, by taking degradation rate data from (J M Gancedo, 1982), and a range of translation rates from (Boehlke and Friesen, 1975) it was possible for us to show that the observed data for the first growth law are fully in line with the prediction of the model (Fig. 3 - Supplement 3).

A combined model accounting for both active ribosomes and protein turnover predicts at most 20% of inactive ribosomes at slow growth

While the data converge on a role of degradation in determining ribosomal fractions at slow growth, this does not by itself exclude that inactive ribosomes may also play a role. The measured degradation rates are generally slightly smaller than model predictions, which could suggest that inactive ribosomes are also present, but their fraction must be

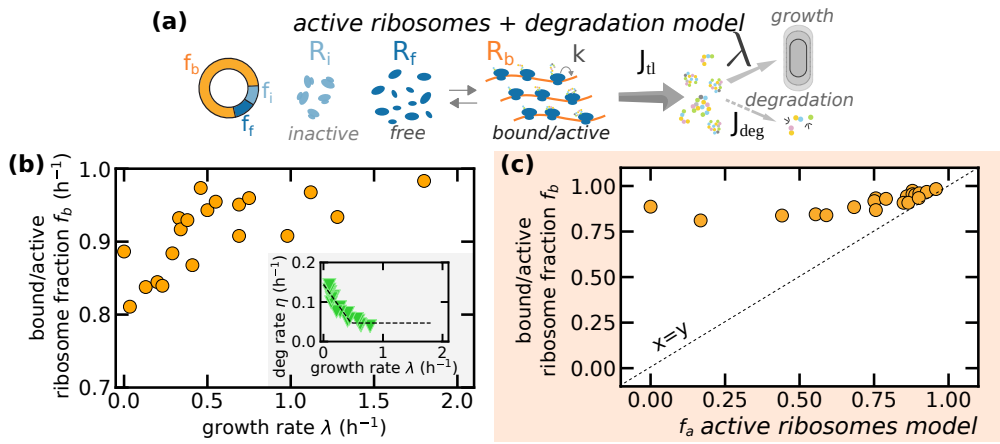


Fig 4. In a picture including degradation, inactive ribosomes are at most a small fraction. (a) Sketch of the combined model where degradation is included and ribosomes can become inactive. (b) Estimated fraction of bound/active ribosome f_b (orange circles) assuming the combined model and using *E. coli* data from (Dai et al., 2016) and degradation data from (Pine, 1973) (shown in the inset). (c) Comparison of estimated fraction of active ribosomes from the standard active ribosomes model (x axis) and the combined model (y axis) using data data from (Dai et al., 2016) (orange circles).

much lower than expected by a framework neglecting protein turnover. To explore this idea, we developed a combined framework considering both features (Fig. 4a).

We now repeat the procedure followed in the degradation model splitting the unbound ribosome pool into free and inactive fractions, as sketched in Fig. 4a. Free ribosomes can bound mRNA (and thus become translationally active). The growth law can be written as:

$$\lambda = \gamma(\phi_R - \phi_R^i) - \eta = \gamma\phi_R f_b - \eta, \quad (13)$$

where both the fraction f_b of bound/active ribosomes and the role of protein turnover are taken into account. It is possible once again to use Equation (13) to infer the fraction of bound/active ribosomes as a function of the growth rate (Fig. 4b) when $\eta(\lambda)$ is known. This reasoning suggests that an increasing fraction of inactive and free ribosomes might still exist at slow growth, but they would be no more than 20% of the total (Fig. 4c).

Finally, we note that in the combined model it is possible to write ϕ_R as a function of the dimensionless parameter $\Lambda := (\lambda + \eta)/\gamma$,

$$\phi_R = \frac{\Lambda}{f_b}, \quad (14)$$

which highlights the relevance of the relative role of the time scales of ribosome production (γ) and dilution/degradation ($\lambda + \eta$) in determining ϕ_R . An ideal experimental setup would be capable of informing on ribosomal mass fraction, protein degradation and elongation rate as functions of the growth rate. This would then give access to the experimental (still indirect) quantification of the bound/active ribosome fraction f_b . Since Eq. (14) is linear in Λ , deviations from linearity would indicate a growth dependence of the fraction of active ribosomes.

Discussion and Conclusions

The concepts of maintenance and turnover are central in biosynthesis, and become particularly relevant for slow-growing cells. It seems natural that they would play a

role in growth laws. While some recent studies on *E. coli* have focused on biomass recycling from dead cells (Schink et al., 2019; Biselli et al., 2020), here we provide a complementary interpretation for the determinants of the “first” growth law relating ribosome fraction to growth rate in different nutrient conditions. The idea that protein degradation would make the relationship between ribosomal sector and growth rate linear but not proportional was first suggested by (Bosdriesz et al., 2015), but this study only commented briefly on this possibility, and did not explore its implications. The concepts introduced here clarify some important aspects on the behavior of slowly-growing *E. coli*. Specifically, data and models converge on a scenario where protein degradation sets a maintenance level of ribosomes at vanishing growth. Inactive ribosomes might play a role, but their relative fraction must be smaller than previously expected, even at vanishing growth. Here, in contrast with the widespread notion that at slow growth the fraction of active ribosome tends to disappear, we suggest that ribosome turnover sets a reservoir of maintenance ribosomes at vanishing growth.

A further question highlighted by our analysis concerns the causes and the mechanistic determinants of the increase in degradation rates observed at slow growth. While classic studies have observed this effect (Goldberg and Dice, 1974; Maurizi, 1992; Pine, 1973), there is no convergence about the biological mechanisms underlying this change. Misfolding and protein aggregation occur when translation is slow (Maurizi, 1992), and one could speculate that enhanced protein degradation contributes to the removal of waste products. Other hypotheses regard protein degradation as a strategy to strengthen the recycling of amino-acids under limited nutrient conditions, or as a post-translational control mechanism that would tune the level of specific proteins (Goldberg and Dice, 1974; Maurizi, 1992; Pine, 1973).

We also remark that the observed increase of the average degradation rate may also result from the variability of the protein mass fractions in different growth regimes. Here, we did not consider protein-specific degradation rates. However, we can establish a minimal framework with degradation rates η_R and η_P that are specific to two corresponding protein sectors ϕ_R and ϕ_P (typically representing a ribosomal and a metabolic sector). Eq.(2) still holds redefining η as

$$\eta := \eta_R \phi_R + \eta_P \phi_P = \eta_P (1 - e \phi_R), \quad (15)$$

i.e. as the weighted average of the degradation rates of the corresponding sectors, with $e := 1 - \eta_R/\eta_P$ and assuming $\phi_R + \phi_P = 1$ for simplicity. Eq. (15) indicates that the growth-dependence of η might also emerge from the variability of the mass fractions ϕ at different physiological states. Unfortunately no experimental data currently allow us to validate this scenario, hence we stuck to the most parsimonious assumption of a common rate. However, we do note that interspecific predictions of the ribosome abundance based on protein abundance and growth rate use this modification and can describe data for diverse species (Kempes et al., 2016). This connection highlights the importance of future work that considers the interplay of shifts in protein abundance, degradation rates, and transcript partitioning across species. We also note that selective degradation of nonribosomal proteins under slow growth has been proposed to play an important role in determining optimal energy efficiency in slow-growing bacteria (Maitra and Dill, 2015).

Beyond *E. coli*, we expect that the concepts developed here should be even more important for our understanding of growth laws in slow-growing bacteria and eukaryotes. In yeast, protein turnover has been quantified precisely (Christiano et al., 2014), and protein-specific and regulatory aspects of protein degradation and turnover are well known. In particular, selective degradation rates for ribosomal and different kinds of metabolic proteins in different regimes have been reported (Martin-Perez and Villén,

2017; Christiano et al., 2014; Belle et al., 2006; Helbig et al., 2011), which should affect the first growth law (Metzl-Raz et al., 2017). Finally, eukaryotic cells have been reported to activate the expression of autophagy proteins at slow growth, also targeting ribosomes (Beese et al., 2020). However, these aspects remain unexplored from the quantitative standpoint. We expect protein turnover to be relevant in other eukaryotic cells, as post-translation control becomes more common in setting protein concentrations; for instance, fibroblasts increase degradation rates of long-lived proteins as they transition from a proliferating to a quiescent state (Zhang et al., 2017).

In conclusion, our results lead us to conclude that protein turnover is needed to explain important features of cellular resource allocation underlying the growth laws, in particular at slow growth, when the time scales of mass loss for protein degradation and dilution become comparable. In such conditions, differential degradation of proteins with different functions and expression levels will likely play a role in determining physiological responses that yet escape our knowledge. A new generation of large-scale studies of protein-specific degradation, starting from *E. coli*, may help us building a condensed and quantitative picture of global cell physiology that includes protein turnover.

Methods and Materials

Models

We discuss three different models throughout this study. The “degradation model” (Box 1) provides the relation $\phi_R(\lambda)$ by considering the contribution of protein degradation - Eq.(2). The “active ribosome” model, leading to Eq.(7), is our formulation of the standard theory that neglects protein turnover (Dai et al., 2016) (Box 2). The third model that we develop in the last section comprises both aspects of the previous theories (protein degradation and existence of a pool of inactive ribosomes) and is obtained by the procedure explained in Box 1 and considering a total number of ribosomes $R = R_f - R_i - R_b$. Thus, Eq.(5) becomes $R_f = k(R - R_i)/(k + Lc_m\alpha_0)$ and, upon the same hypotheses explained in Box 1, it leads to Eq. (13).

Data sets

Growth rate and protein mass fraction

We used data from Metzl-Raz et al. (2017) (*S. cerevisiae*), Dai et al. (2016) (*E. coli*), Fraenkel and Neidhardt (1961) (*A. aerogenes*), Alberghina et al. (1975) (*N. crassa*), Brown and Rose (1969) (*C. utilis*), Cook (1963) (*E. gracilis*) in Figures 3, 1 - Supplement 1 and 3 - Supplement 3.

Experimental data

We compiled two data sets from the literature relative to degradation rates in *E. coli* and *S. cerevisiae*. These data are available as a Mendeley Data repository at the following address <http://dx.doi.org/10.17632/85pxpdsx38.1>.

For *E. coli*, we considered data of the average protein degradation rate from (Pine, 1970; Nath and Koch, 1970; Pine, 1973; Mosteller et al., 1980; Larrabee et al., 1980; J M Gancedo, 1982). For *S. cerevisiae*, we considered data from (J M Gancedo, 1982; Helbig et al., 2011; Christiano et al., 2014; Martin-Perez and Villén, 2017). These studies can be divided into two categories according to their experimental design:

1. studies that provide a distribution of degradation rates by measuring the half-life of hundreds or thousands of proteins. Out of these studies, we estimated the mean degradation rate as the average of this distribution. In *E. coli*, (Mosteller et al., 1980; Larrabee et al., 1980) provide a distribution of degradation rates by combining pulse-chase experiments with 2-D gel electrophoresis. We note that these authors measure ≈ 100 degradation rates, but there are more than 4000 *E. coli* proteins. In *S. cerevisiae*, (Helbig et al., 2011; Christiano et al., 2014; Martin-Perez and Villén, 2017) measure the half-lives of thousands of protein by combining metabolic labelling and mass spectrometry. (Christiano et al., 2014; Martin-Perez and Villén, 2017) perform SILAC experiments, which are based on amino acid labelling, while (Helbig et al., 2011) use stable heavy nitrogen isotopes for labelling. We note that in figure 3 - Supplement 3 we have excluded the estimate of the mean degradation rate obtained from (Christiano et al., 2014) since it is an order of magnitude higher than other studies. This discrepancy is also pointed out by (Martin-Perez and Villén, 2017) who partially ascribe it to protocol differences. Finally, we also note that in figure 3 - Supplement 3 we show only one data point from (Martin-Perez and Villén, 2017), but these authors actually perform two further degradomics experiments in different growth conditions. We did not include such data points because they find a mean degradation rate 4-8 times greater than other studies at similar growth rates. We believe that this discrepancy may be due to sampling bias: while the main experiment of (Martin-Perez and Villén, 2017) (shown in figure 3 - Supplement 3) measures degradation rates for ≈ 3000 proteins, , in these two experiments they measure ≈ 1800 proteins. As a consequence there may be sub-sampling of long-lived proteins that increases the observed mean degradation rate.
2. studies that measure total protein content breakdown and use data analysis to infer the mean degradation rate. All such studies never measure directly the degradation dynamics of specific proteins, but only the dynamics of total protein content. In *E. coli*, (Pine, 1970; Nath and Koch, 1970; Pine, 1973) provide a single mean degradation rate. Nath and Koch (1970) also attempts to estimate the rate of two distinct protein classes, respectively fast-degrading and slow-degrading types. In *S. cerevisiae*, (J M Gancedo, 1982) uses the same type of set-up. All these studies perform pulse-chase experiments by labelling completely the proteome of the cell by incorporation of radioactively-labelled amino acids. After switching to incorporation of unlabelled amino acids, the total amount of labelled protein can either stay constant or decrease due to degradation. For all these studies, we performed our own data analysis on the the provided raw data and estimated the mean degradation rate from the rate of decrease of the labelled total cell protein. We describe below the methods of our data analysis.

Data analysis

We begin this section by considering the work of Pine (1973), our main source in the main text for degradation rates across growth conditions. In this case, we have followed the author's estimates since the raw data are provided only for few conditions, but we have re-examined critically their assumption. The authors estimate the mean degradation rate by assuming that the labelled cell protein decreases with a single degradation rate. Mathematically, this means that

$$P_L(t) = P_L^0 \cdot \exp(-\eta \cdot t) , \quad (16)$$

with $P_L(t)$ being the amount of labelled protein at time t after the pulse period. This allows to estimate η as

$$\eta = -\frac{1}{t} \log \left(\frac{P_L(t)}{P_L^0} \right), \quad (17)$$

or any equivalent combination. We note that this method provides a good estimate even if the degradation rate differs from protein to protein. To see this, we re-write equation (16):

$$P_L(t) = \sum_i P_{Li}^0 \cdot \exp(-\eta_i t) \quad (18)$$

where the sum runs over all the proteins in the cell. By considering the initial fraction of proteins having degradation rate η , we can write this in terms of the distribution $P(\eta)$.

$$\log \left(\frac{P_L(t)}{P_L^0} \right) = \int P(\eta) \exp(-\eta t) d\eta = \langle \exp(-\eta t) \rangle, \quad (19)$$

where the sign $\langle \cdot \rangle$ indicates performing an average.

Since approximately

$$\langle \exp(-\eta t) \rangle \approx \exp(-\langle \eta \rangle t), \quad (20)$$

the previous equation still holds in the mean,

$$\langle \eta \rangle \approx -\log \left(\frac{P_L(t)}{P_L^0} \right) \frac{1}{t}. \quad (21)$$

Jensen's inequality implies that this estimate always underestimates the true mean degradation rate, hence, the experimental data points shown in Fig. 3 could be considered as lower bounds.

For (Nath and Koch, 1970; Pine, 1970), we estimated the mean degradation by the dividing the cell protein content in three classes, one of which consists of stable proteins. The other two classes represent respectively fast and slow degrading proteins. This approach is directly inspired by the ideas of (Nath and Koch, 1970).

The total protein content will decay in general according to the following equation:

$$P_L(t) = P_{\text{fast}}^0 \cdot \exp(-\eta_{\text{fast}} t) + P_{\text{slow}}^0 \cdot \exp(-\eta_{\text{slow}} t) + P_{\text{stable}}^0 \quad (22)$$

or as a fraction of initial amount of labelled protein

$$\frac{P_L(t)}{P_L^0} = f_{\text{fast}} \cdot \exp(-\eta_{\text{fast}} t) + f_{\text{slow}} \cdot \exp(-\eta_{\text{slow}} t) + f_{\text{stable}} \quad (23)$$

with f_{fast} , f_{slow} and f_{stable} being the probability that a protein belongs to one of the three classes.

The mean degradation rate will be:

$$\langle \eta \rangle = f_{\text{fast}} \eta_{\text{fast}} + f_{\text{slow}} \eta_{\text{slow}} \quad (24)$$

To estimate this, we must infer the parameters f_{fast} , η_{fast} , f_{slow} and η_{slow} from equation (23). In practice, we are able to reduce the number of parameters on a case-by-case basis.

(Nath and Koch, 1970) and (J M Gancedo, 1982) perform this analysis themselves, and assume that the slow class is indeed slow enough to approximate the exponential to a linear function. They derive equation (23) and obtain:

$$-\frac{1}{P_L^0} \frac{dP_L(t)}{dt} = f_{\text{fast}} \eta_{\text{fast}} \cdot \exp(-\eta_{\text{fast}} t) + f_{\text{slow}} \eta_{\text{slow}} \quad (25)$$

They fit f_{fast} , η_{fast} and $f_{\text{slow}} \cdot \eta_{\text{slow}}$ to the experimental curve. We are able to extract the mean degradation rate out of these parameters.

(Pine, 1970) do not perform this analysis. By performing it ourselves, we find that using only two classes fits the data well using the following expression:

$$\frac{P_L(t)}{P_L^0} = f_{\text{fast}} \cdot \exp(-\eta_{\text{fast}}t) + (1 - f_{\text{fast}}) \quad (26)$$

We extract f_{fast} and η_{fast} from the fit and use it to compute the mean degradation rate.

Table 1. Summary of the symbols used in the text.

Symbol	Definition
M	total protein mass
M_R	total ribosomal protein mass
$\phi_R = M_R/M$	mass fraction of ribosomal proteins
λ	growth rate
J_{tl}	mass translational flux
m_p	typical protein mass
m_R	protein mass of a ribosome
R_b	number of transcript-bound ribosomes
R_a	number of active ribosomes
R_i	number of inactive ribosomes
R_f	number of free ribosomes, available to bind the mRNA
$R = R_i + R_f + R_b$	total number of ribosomes in our framework
$R = R_i + R_a$	total number of ribosomes in the standard framework
k	codon elongation rate
L_R	total number of aa in a ribosome
$\gamma = k/L_R$	inverse of typical time to translate all amino-acids of a ribosome
$\phi_R = M_R/M = m_R R/M$	protein mass fraction of ribosomal proteins

Acknowledgments

MCL and LCa are funded by the Italian Association for Cancer Research AIRC-IG (REF: 23258), and LCa by was funded by the AIRC Fellowship (REF: 23870).

MO is supported by the Departments of Excellence 2018-2022 Grant awarded by the Italian Ministry of Education, University and Research (MIUR) (Grant No. L. 232/2016)

References

- Alberghina, F., Sturani, E., and Gohlke, J. (1975). Levels and rates of synthesis of ribosomal ribonucleic acid, transfer ribonucleic acid, and protein in *neurospora crassa* in different steady states of growth. *Journal of Biological Chemistry*, 250(12):261–272.
- Beese, C. J., Brynjólfssdóttir, S. H., and Frankel, L. B. (2020). Selective Autophagy of the Protein Homeostasis Machinery: Ribophagy, Proteaphagy and ER-Phagy. *Frontiers in Cell and Developmental Biology*, 7(January):1–12.
- Belle, A., Tanay, A., Bitincka, L., Shamir, R., and O’Shea, E. K. (2006). Quantification of protein half-lives in the budding yeast proteome. *Proceedings of the National Academy of Sciences*, 103(35):13004–13009.

- Biselli, E., Schink, S. J., and Gerland, U. (2020). Slower growth of *Escherichia coli* leads to longer survival in carbon starvation due to a decrease in the maintenance rate. *Molecular systems biology*, 16:e9478.
- Boehlke, K. W. and Friesen, J. D. (1975). Cellular content of ribonucleic acid and protein in *Saccharomyces cerevisiae* as a function of exponential growth rate: calculation of the apparent peptide chain elongation rate. *Journal of Bacteriology*, 121(2):429–433.
- Borkowski, O., Ceroni, F., Stan, G. B., and Ellis, T. (2016). Overloaded and stressed: whole-cell considerations for bacterial synthetic biology. *Current Opinion in Microbiology*, 33:123–130.
- Bosdriesz, E., Molenaar, D., Teusink, B., and Bruggeman, F. J. (2015). How fast-growing bacteria robustly tune their ribosome concentration to approximate growth-rate maximization. *The FEBS Journal*, 282(10):2029–2044.
- Brown, C. M. and Rose, A. H. (1969). Effects of temperature on composition and cell volume of *Candida utilis*. *Journal of Bacteriology*, 97(1):261–272.
- Christiano, R., Nagaraj, N., Fröhlich, F., and Walther, T. C. (2014). Global proteome turnover analyses of the yeasts *S. cerevisiae* and *S. pombe*. *Cell Reports*, 9(5):1959–1965.
- Ciandrini, L., Stansfield, I., and Romano, M. C. (2013). Ribosome traffic on mRNAs maps to gene ontology: Genome-wide quantification of translation initiation rates and polysome size regulation. *PLoS Comput. Biol.*, 9.
- Cook, J. R. (1963). Adaptations in growth and division in *Euglena* effected by energy supply*. *The Journal of Protozoology*, 10(4):436–444.
- Dai, X. and Zhu, M. (2020). Coupling of ribosome synthesis and translational capacity with cell growth. *Trends in biochemical sciences*, 45:681–692.
- Dai, X., Zhu, M., Warren, M., Balakrishnan, R., Patsalo, V., Okano, H., Williamson, J. R., Fredrick, K., Wang, Y.-P., and Hwa, T. (2016). Reduction of translating ribosomes enables *Escherichia coli* to maintain elongation rates during slow growth. *Nature microbiology*, 2:16231.
- DeLong, J. P., Okie, J. G., Moses, M. E., Sibly, R. M., and Brown, J. H. (2010). Shifts in metabolic scaling, production, and efficiency across major evolutionary transitions of life. *Proceedings of the National Academy of Sciences*, 107(29):12941–12945.
- Fraenkel, D. G. and Neidhardt, F. C. (1961). Use of chloramphenicol to study control of rna synthesis in bacteria. *Biochimica et Biophysica Acta*, 53(1):96 – 110.
- Gefen, O., Fridman, O., Ronin, I., and Balaban, N. Q. (2014). Direct observation of single stationary-phase bacteria reveals a surprisingly long period of constant protein production activity. *Proceedings of the National Academy of Sciences*, 111(1):556–561.
- Goldberg, A. and Dice, J. (1974). Intracellular protein degradation in mammalian and bacterial cells. *Annual Review of Biochemistry*, 43(1):835–869. PMID: 4604628.
- Gray, D. A., Dugar, G., Gamba, P., Strahl, H., Jonker, M. J., and Hamoen, L. W. (2019). Extreme slow growth as alternative strategy to survive deep starvation in bacteria. *Nature Communications*, 10.

- Greulich, P., Ciandrini, L., Allen, R. J., and Romano, M. C. (2012). Mixed population of competing totally asymmetric simple exclusion processes with a shared reservoir of particles. *Phys. Rev. E*, 85.
- Helbig, A. O., Daran-Lapujade, P., van Maris, A. J. A., de Hulster, E. A. F., de Ridder, D., Pronk, J. T., Heck, A. J. R., and Slijper, M. (2011). The diversity of protein turnover and abundance under nitrogen-limited steady-state conditions in *saccharomyces cerevisiae*. *Mol. BioSyst.*, 7:3316–3326.
- J M Gancedo, S López, F. B. (1982). Calculation of half-lives of proteins in vivo. heterogeneity in the rate of degradation of yeast proteins. *Molecular and Cellular Biochemistry*, 43(89-95):436–444.
- Kafri, M., Metzl-Raz, E., Jonas, F., and Barkai, N. (2016). Rethinking cell growth models. *FEMS yeast research*, 16.
- Kempes, C. P., van Bodegom, P. M., Wolpert, D., Libby, E., Amend, J., and Hoehler, T. (2017). Drivers of bacterial maintenance and minimal energy requirements. *Frontiers in microbiology*, 8:31.
- Kempes, C. P., Wang, L., Amend, J. P., Doyle, J., and Hoehler, T. (2016). Evolutionary tradeoffs in cellular composition across diverse bacteria. *The ISME journal*, 10:2145–2157.
- Klumpp, S., Scott, M., Pedersen, S., and Hwa, T. (2013). Molecular crowding limits translation and cell growth. *Proceedings of the National Academy of Sciences of the United States of America*, 110:16754–16759.
- Larrabee, K. L., Phillips, J. O., Williams, G. J., and Larrabee, A. R. (1980). The relative rates of protein synthesis and degradation in a growing culture of *escherichia coli*. *Journal of Biological Chemistry*, 255(9):4125–30.
- Li, G. W. (2015). How do bacteria tune translation efficiency? *Current Opinion in Microbiology*, 24:66–71.
- Long, A. M., Hou, S., Ignacio-Espinoza, J. C., and Fuhrman, J. A. (2021). Benchmarking microbial growth rate predictions from metagenomes. *The ISME journal*, 15(1):183–195.
- Maitra, A. and Dill, K. A. (2015). Bacterial growth laws reflect the evolutionary importance of energy efficiency. *Proceedings of the National Academy of Sciences of the United States of America*, 112:406–411.
- Martin-Perez, M. and Villén, J. (2017). Determinants and regulation of protein turnover in yeast. *Cell Systems*, 5(3):283–294.e5.
- Maurizi, M. (1992). Proteases and protein degradation in *escherichia coli*. *Experientia*, 48(2):178–201.
- Metzl-Raz, E., Kafri, M., Yaakov, G., Soifer, I., Gurvich, Y., and Barkai, N. (2017). Principles of cellular resource allocation revealed by condition-dependent proteome profiling. *eLife*, 6.
- Mosteller, R. D., Goldstein, R. V., and Nishimoto, K. R. (1980). Metabolism of individual proteins in exponentially growing *escherichia coli*. *The Journal of biological chemistry*, 255(6):2524—2532.

- Nath, K. and Koch, A. L. (1970). Protein degradation in escherichia coli: I. measurement of rapidly and slowly decaying components. *Journal of Biological Chemistry*, 245(11):2889–2900.
- Nath, K. and Koch, A. L. (1971). Protein degradation in escherichia coli : Ii. strain differences in the degradation of protein and nucleic acid resulting from starvation. *Journal of Biological Chemistry*, 246(22):6956–6967.
- Pine, M. J. (1970). Steady-state measurement of the turnover of amino acid in the cellular proteins of growing escherichia coli: Existence of two kinetically distinct reactions. *Journal of Bacteriology*, 103(1):207–215.
- Pine, M. J. (1973). Regulation of intracellular proteolysis in escherichia coli. *Journal of bacteriology*, 115(1):107–116.
- Santra, M., Farrell, D. W., and Dill, K. A. (2017). Bacterial proteostasis balances energy and chaperone utilization efficiently. *Proceedings of the National Academy of Sciences of the United States of America*, 114:E2654–E2661.
- Schink, S. J., Biselli, E., Ammar, C., and Gerland, U. (2019). Death rate of e. coli during starvation is set by maintenance cost and biomass recycling. *Cell systems*, 9:64–73.e3.
- Schroer, D. W. and St. John, A. C. (1981). Relative stability of membrane proteins in escherichia coli. *Journal of Bacteriology*, 146(2):476–483.
- Scott, M. and Hwa, T. (2011). Bacterial growth laws and their applications. *Current opinion in biotechnology*, 22:559–565.
- Scott, M., Mateescu, E. M., Zhang, Z., and Hwa, T. (2010). Interdependence of Cell Growth Origins and Consequences. *Science*, 330(November):1099–1102.
- Shaw, L. B., Zia, R. K., and Lee, K. H. (2003). Totally asymmetric exclusion process with extended objects: a model for protein synthesis. *Phys. Rev. E*.
- Zhang, T., Wolfe, C., Pierle, A., Welle, K. A., Hryhorenko, J. R., and Ghaemmaghani, S. (2017). Proteome-wide modulation of degradation dynamics in response to growth arrest. *Proceedings of the National Academy of Sciences of the United States of America*, 114:E10329–E10338.
- Zhu, M., Mu, H., Jia, M., Deng, L., and Dai, X. (2020). Control of ribosome synthesis in bacteria: the important role of rrna chain elongation rate. *Science China. Life sciences*.

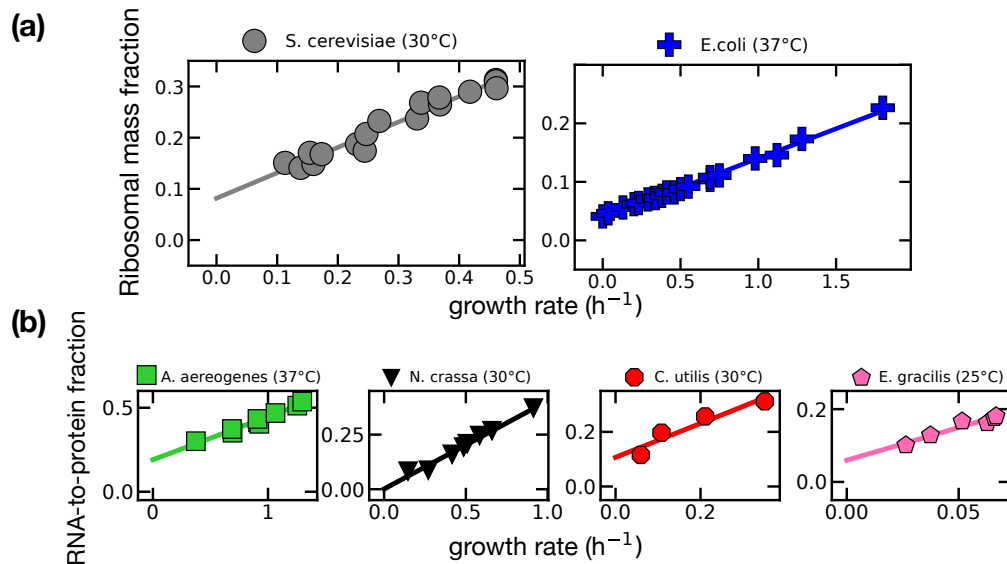


Fig 1 - Supplement 1. The first growth law typically shows an offset in data. (a) Data on ribosomal mass fraction for *E. coli* and *S. cerevisiae*. (b) Data on RNA/protein ratios for other organisms. Data from Metzler-Raz et al. (2017) (*S. cerevisiae*), Dai et al. (2016) (*E. coli*), Fraenkel and Neidhardt (1961) (*A. aerogenes*), Alberghina et al. (1975) (*N. crassa*), Brown and Rose (1969) (*C. utilis*), Cook (1963) (*E. gracilis*).

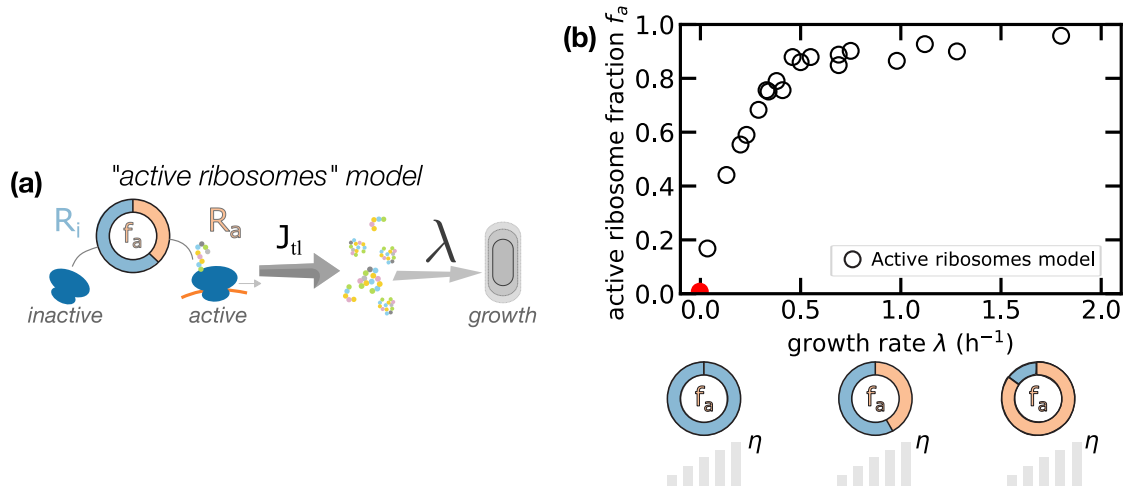


Fig 3 - Supplement 1. (a) In the standard framework ribosomes are divided in two categories - active and inactive - and only the fraction f_a of active ribosomes is responsible for protein production. (b) The plot reports the estimated f_a (circles) assuming this model and using data from Dai et al. (2016). The red circle represents the extrapolated point at zero growth.

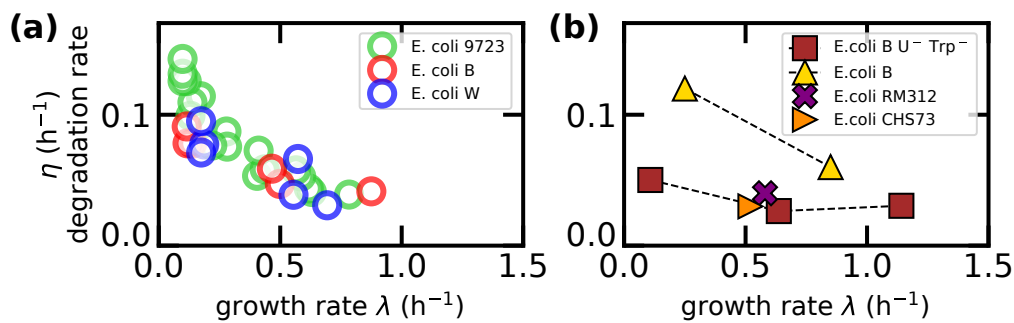


Fig 3 - Supplement 2. (a) Degradation rate across growth conditions from Pine (1973) as used in the main text. (b) Degradation rate across different growth conditions from other studies using different strains and techniques, Nath and Koch (1970) (*E. coli* B $U^{-1} \text{Trp}^{-}$), Pine (1970) (*E. coli* B), Mosteller et al. (1980) (*E. coli* RM132), Larrabee et al. (1980) (*E. coli* CHS73).

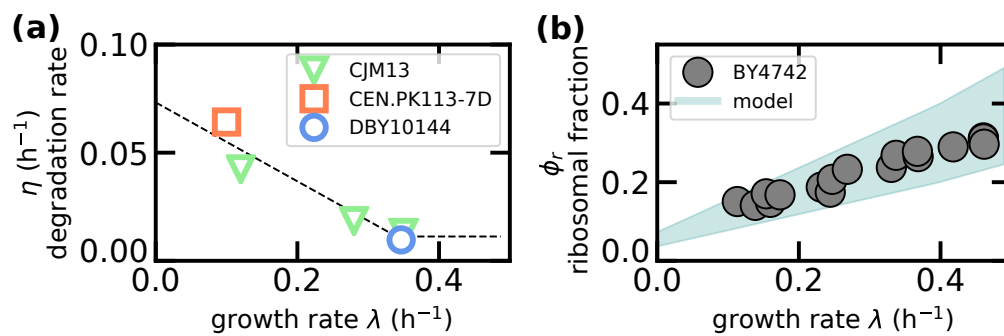


Fig 3 - Supplement 3. The degradation model is in line with data for *S. cerevisiae*. (a) Mean degradation rate across growth conditions from (J M Gancedo, 1982), (Helbig et al., 2011), (Martin-Perez and Villén, 2017), respectively using strains CJM13, CEN.PK113-7D and DBY10144. The dashed line indicates a linear fit to these data. (b) The range of predicted ribosomal fractions of the model, plotted next to data points from (Metzl-Raz et al., 2017) which uses strain BY4742. The model requires as input degradation rates and translation elongation rates. We have taken the linear fit from panel a and used it to extrapolate degradation rates to the growth rates measured by (Metzl-Raz et al., 2017). We then considered a range of physiologically relevant translation elongation rates (3-8 aa s^{-1}) from ref. (Boehlke and Friesen, 1975). The shaded area represents the prediction of the model for such range.